



**HAL**  
open science

# Holistic Approach for Aircraft Trajectory Optimization Using Optimal Control

Hasnae Kasmi, Serge Laporte, Marcel Mongeau, Andrija Vidosavljevic, Daniel  
Delahaye

► **To cite this version:**

Hasnae Kasmi, Serge Laporte, Marcel Mongeau, Andrija Vidosavljevic, Daniel Delahaye. Holistic Approach for Aircraft Trajectory Optimization Using Optimal Control. *Journal of Aircraft*, 2023, pp.1-12. 10.2514/1.C036784 . hal-04049261

**HAL Id: hal-04049261**

**<https://hal-enac.archives-ouvertes.fr/hal-04049261>**

Submitted on 31 Mar 2023

**HAL** is a multi-disciplinary open access archive for the deposit and dissemination of scientific research documents, whether they are published or not. The documents may come from teaching and research institutions in France or abroad, or from public or private research centers.

L'archive ouverte pluridisciplinaire **HAL**, est destinée au dépôt et à la diffusion de documents scientifiques de niveau recherche, publiés ou non, émanant des établissements d'enseignement et de recherche français ou étrangers, des laboratoires publics ou privés.

# Holistic approach for aircraft trajectory optimization using optimal control

Hasnae Kasmi \* and Serge Laporte †

*Airbus, France*

*University Paul Sabatier, University of Toulouse, France*

Marcel Mongeau ‡, Andrija Vidosavljevic §, Daniel Delahaye ¶

*ENAC, University of Toulouse, France*

This paper deals with an optimal control approach for commercial aircraft trajectory planning, focusing on the vertical path and the minimization of the fuel burned. The main contribution is the optimization of the whole trajectory, also called the *mission*, without prior separation into different flight phases (climb, cruise, and descent), contrary to traditional approaches that consider the flight phases sequentially. The proposed Optimal Control Problem (OCP) is formulated, and then solved using a direct collocation method. Initial results yield optimal trajectories with a gradual climb during the cruise (climb cruise), which correspond to theoretical trajectories that minimize fuel consumption. Furthermore, a penalization is introduced to ensure vertical profiles featuring horizontal cruise levels on so-called *flight levels*, compliant with current Air Traffic Management (ATM) regulations. The use of direct methods to address this OCP induces large non-linear optimization problems that we solve using an interior point method. This methodology is likely to lead to poor local optima but a simple multi-start heuristic shows that the solutions found for standard problems appear to be globally optimal. Such an approach does not need to impose *a priori* the cruise flight levels, and is suitable for commercial aircraft flight planning purposes. It leads to fuel saving and subsequently to important improvements against environmental impact by reducing  $CO_2$  emissions.

## I. Introduction

AVIATION transport is considered as a significant contributor of the pollution problem on Earth. Before the COVID-19 pandemic, air traffic accounted for 24% of nitrogen oxides ( $NO_x$ ) emissions [1]. The International Civil Aviation Organization (ICAO) suggests that 13% of carbon dioxide ( $CO_2$ ) emissions in the transport industry are linked to aircraft operations, which corresponds to 2% of the total  $CO_2$  released into the atmosphere. Contrails and noise

---

\*PhD student, IGFX, hasnae.kasmi@airbus.com.

† Aircraft performance engineer, IGFX, serge.laporte@airbus.com.

‡ Professor, mongeau@recherche.enac.fr.

§ Assistant Professor, vidosavljevic@recherche.enac.fr.

¶ Professor, delahaye@recherche.enac.fr.

have also their impact on the environment [2–4]. The rate of increase of these amounts is linked to the volume of air traffic and to the aviation services that are increasing, as reported by the International Air Transport Association (IATA). In order to address these environmental issues, beside others such as capacity and safety, two major programs have been developed: SESAR [5] in Europe and NextGen [6] in North America. Their objective is to implement the Trajectory Based Operation (TBO) paradigm by allowing airlines to plan more flexibly their trajectories, making possible more efficient flights closer to the airlines needs [7]. In this context, airlines may exploit such a relaxation of operational constraints to optimize their flight plans, and eventually consider ATM network restrictions during business trajectory negotiation processes [8, 9].

The trajectory optimization problem is classically divided into a series of so-called guiding subproblems dealing with predefined flight phases: take-off [10], climb [11, 12], cruise [13], descent [14–19], approach [20, 21], and landing [22]. This decomposition is historically justified by the structure of aircraft systems (aerodynamics configurations, engine ratings) and also by the operational procedures that change from phase to phase. Some research studies consider the whole aircraft trajectory, and model the problem as a multi-phase trajectory optimization problem [23–27]. A major difficulty of addressing such a multi-phase optimization problem is the management of the transition between phases, which is classically modeled with large-scale mixed-integer nonlinear optimization problems involving thereby prohibitive combinatorics. In this paper, we overcome this difficulty by proposing a unified formulation that describes the dynamics of the aircraft with a single set of equations for all phases (climb, cruise and descent), and considering a unique set of control parameters for the whole mission. The different flight phases are not introduced *a priori*: they naturally emerge from a penalty that models the operational needs. The initial difficulty induced by the classical mixed-integer problem is then shifted into another kind of difficulty: dealing with a strongly non-convex objective function.

## II. Related work and contributions

Trajectory optimization of commercial flights is a long-term research focus in civil aviation. Since the 60s, many effective and comprehensive implementations of flight trajectory optimization techniques were studied to enhance the sustainability of aircraft operations both in short- and long-haul travels. The work of Bryson and Hedrick is one of the first studies that deal with the three-dimensional optimization problem [28] using the energy state approximation defined by the combination of height and speed to reduce the problem size. Many other interesting researches focus on this field from an energy point of view, see for instance [29–33].

Last decades have been characterized by a renewed interest in aircraft trajectory optimization due to technology enhancement. A wide bunch of path-planning tools have been proposed for this purpose, including dynamic programming approaches [34], optimal control techniques [35], heuristic and meta-heuristic methods and path-planing algorithms [36, 37]. Hargraves and Paris carry out a study about climb trajectory optimization by using direct collocation methods

to transform the Optimal Control Problem (OCP) into a nonlinear optimization problem [38]. The resulting Nonlinear Programming Problem (NLP) is solved with a sequential quadratic programming (SQP) method. Visser has also given interest to this kind of problem in the context of 4D time-based operations [39].

Other works consider the problem as a multi-phase optimal control problem applying various numerical methods to solve it [23, 35, 40]. Betts *et al.* divide the aircraft trajectory optimization problem into a series of subproblems that are solved using indirect methods [41]. Other methods to solve OCPs include techniques based on the Pontryagin minimum principle and the Hamiltonian-Jacobi-Bellman equation [42]. Villarroel and Rodrigues [43] also apply an optimal control approach to minimize the operating costs during the climb and descent phases managed by the Flight Management System (FMS). Soler *et al.* performed significant research on aircraft trajectory optimization: they address a multiphase hybrid trajectory optimization in [44], and subsequently investigate a multiphase commercial aircraft trajectory in a stationary wind field by modeling it as a Mixed-Integer Nonlinear Programming Problem (MINLP) in [45]. Indirect methods are implemented to solve the multi-phase optimal control problem proposed in [16], whose results are compared with trajectories calculated by the FMS under various wind conditions [17]. Gonzalez-Arribas *et al.* address in [46–49] a robust optimal trajectory planning problem under wind and convective weather uncertainties using stochastic optimal control. Direct collocation method is used in [19] to transform the optimal control formulation proposed for the optimization of the descent phase.

Dynamic programming is also applied to aircraft trajectory optimization [34]. Le Merrer uses a direct collocation approach and inverse dynamic programming to optimize the flight trajectory [50]. The results obtained by both methods are comparable. Andreu Altava *et al.* have developed an A\* algorithm in [14, 20, 21] to optimize aircraft trajectories in descent and approach phases. A branch and bound method is used in [51] to solve effectively the problem of optimal trajectory planning subject to obstacle constraints. A genetic algorithm is applied in [52] to address a multi-objective aircraft optimization problem. Girardet *et al.* [53] consider a wind-optimal planning problem with constant speed and solve it with an ordered-upwind algorithm. More detail on mathematical models for trajectory design and OCP resolution methods can be found in [36].

All these studies on commercial aircraft trajectory optimization focus on optimizing only a part of the mission, or consider the optimization of a complete mission as a multiphase problem which leads to large-scale nonlinear optimization problems or large mixed-integer nonlinear optimization problems. Moreover, all multiphase approaches require the *a priori* knowledge of the number of cruise flight levels. To overcome this drawback, we propose a unified formulation that describes the dynamics of the aircraft via a single set of equations. This allows one to replace the multiphase formulation by a monophasic one (still considering climb, cruise and descent), thereby reducing the size of the NLP problem, avoiding the use of integer variables without assuming the number of flight levels.

This method is first validated by a well-known result: the climb cruise [54, 55]. The resulting trajectories will then be used as initial solutions for the second part of the study where we consider the operational requirement of

finding trajectories featuring cruise at predefined cruise levels. To this end, we introduce a penalty approach. As a result we obtain a new optimal control formulation, which is then solved by means of a direct collocation method to obtain trajectories that are suitable to commercial aircraft flight planning purposes.

### III. Problem statement

Traditionally, the trajectory of an aircraft between the departure airport and the destination airport is composed of several flight *phases* [56] which describe the vertical profile (see Figure 1):

**Climb:** The climb phase begins at altitude 10,000 feet (ft) and 250 knots (kt). It is currently implemented with a *CAS/Mach procedure* which splits the climbing phase in two parts: the first one is an arc at constant *Calibrated AirSpeed* (CAS), and the second one at constant *Mach* number. This procedure is commonly considered as a rough approximation of the real optimal speed law that minimizes a *cost*, defined as a convex combination of the time to climb and the fuel consumption [11].

**Cruise:** The cruise phase begins at an altitude called *Top Of Climb* (TOC). It is made of constant altitude/local optimum Mach segments, linked with short CAS/Mach climbs or descents.

**Descent:** The descent phase is performed with a *Mach/CAS* speed law, opposite to climb, until 10,000 ft and 250 kt are reached.

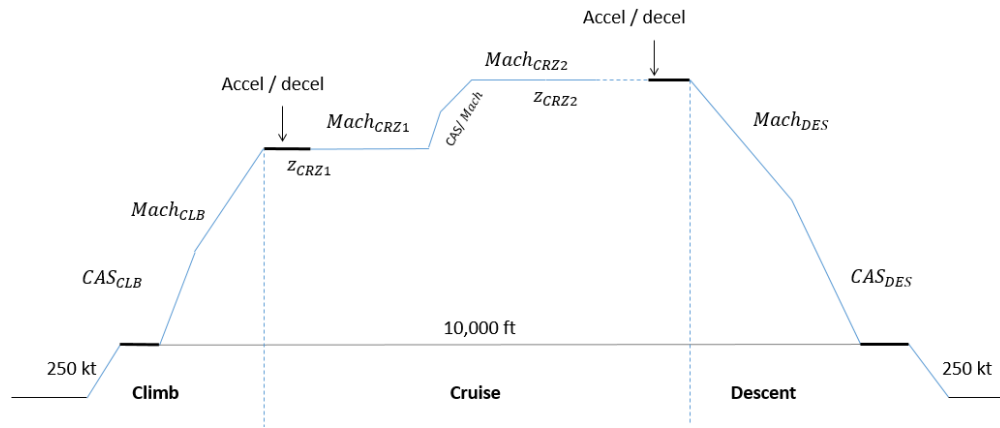


**Fig. 1 Mission profile: the three phases (climb, cruise and descent) and associated speed law**

This paper deals with the optimization of commercial aircraft trajectory planning, focusing on the vertical path and the minimization of the fuel burned. Our aim is to address the whole mission without dividing it *a priori* into several phases. For this purpose, the cruise phase is considered as a particular case of climb and descent phases with null slope, and therefore the complete trajectory is described with a unique set of equations.

## A. Physical model

The aircraft motion equations are based on a point-mass model. They are derived from the fundamental principle of dynamics under the classical simplifying assumptions: flat and non-rotating Earth, small angle of attack, negligible path angle variation, symmetric and coordinated flight (null sideslip), constant heading angle, bank angle neglected, standard atmosphere and no wind. More precisely, we have:

$$F_N - \frac{1}{2}\rho v^2 S_{ref} C_x - mg_0 \sin \gamma = m\dot{v} \quad (1)$$

$$\frac{1}{2}\rho v^2 S_{ref} C_z - mg_0 \cos \gamma = 0, \quad (2)$$

where  $F_N$  is the net thrust,  $C_x$  is the drag coefficient,  $C_z$  is the lift coefficient,  $\rho$  is the air density,  $m$  is the mass,  $v$  is the True AirSpeed (TAS),  $\gamma$  is the aerodynamic path angle,  $g_0$  is the acceleration of gravity, and  $S_{ref}$  is the aerodynamic reference surface of the wing.

These equations are completed with the following kinematic equations:

$$\dot{z} = v \sin \gamma \quad (3)$$

$$\dot{s} = v \cos \gamma, \quad (4)$$

where  $z$  is the altitude and  $s$  is the longitudinal distance along the path.

### Atmospheric model

We use the International Standard Atmosphere (ISA) model to represent the atmosphere. The temperature,  $T_s$ , the pressure,  $P_s$ , the air density,  $\rho$ , and the speed of sound,  $c$ , are described as smooth functions of the pressure altitude,  $Z_p$ . The atmosphere equations are:

$$\left\{ \begin{array}{l} T_s(Z_p) = \begin{cases} T_0 + L_Z Z_p, & \text{for } Z_p \leq Z_{p_{trop}} \\ T_1, & \text{for } Z_p > Z_{p_{trop}} \end{cases} \\ P_s(Z_p) = \begin{cases} P_0 \left( \frac{T_0 + L_Z Z_p}{T_0} \right)^{\alpha_0}, & \text{for } Z_p \leq Z_{p_{trop}} \\ P_1 \exp\left(-\frac{g_0(Z_p - Z_{p_{trop}})}{RT_1}\right), & \text{for } Z_p > Z_{p_{trop}} \end{cases} \\ \rho(Z_p) = \frac{P_s(Z_p)}{RT_s(Z_p)} \\ c(Z_p) = \sqrt{\kappa RT_s(Z_p)}, \end{array} \right. \quad (5)$$

where the couples  $(T_0, P_0)$  and  $(T_1, P_1)$  are the standard temperature and pressure respectively at sea level and at the

tropopause altitude,  $Z_{trop} = 11,000$  m,  $R$  is the perfect gas constant for air,  $L_Z$  is the temperature gradient with the altitude below the tropopause, and  $\kappa$  is the ratio of specific heats for air. Due to the assumptions of ISA atmosphere and constant gravity, we consider the geometric altitude,  $z$ , to coincide with the pressure altitude,  $Z_p$ .

### Performance model

BADA (Base of Aircraft Data) is an aircraft performance model developed by EUROCONTROL [57] for ATM (Air Traffic Management) purposes. It contains several submodels that describe fuel consumption, thrust, aerodynamics, and performance limitations for all supported types of aircraft. However, BADA's accuracy is limited as the model is not based on dedicated flight test data. Nevertheless, it is composed of simple and easily manageable equations that allow the representation of essential aircraft performance behavior. For these reasons, this model is commonly used by the research community, particularly in aircraft trajectory optimization [23, 44, 48].

In our study, we use a BADA model for the aircraft description, with the following simplifications:

- The part of mission we consider (above 10,000 ft) does not require slat/flaps effects on the drag polar.
- The drag polar we consider does not take into account the compressibility effects that occur at high Mach numbers: it is compliant with BADA 3 but not with BADA 4.
- During climb, cruise, and descent, the thrust is assumed to range between Minimum IDle (MID) and Max CLimb (MCL) thrusts. Note that the actual maximum thrust in cruise is lower than MCL, but this limitation is not directly linked to engine considerations: it is specific to the flight management system and solely introduced to reduce engine wear. For that reason we do not consider it here.
- The *specific consumption* (ratio of thrust on fuel-mass flow) is supposed to be constant.

This leads to the following simplified model:

$$C_x = C_{x_0} + kC_z^2 \quad (6)$$

$$F_N = F_{NMID} + \lambda(F_{NMCL}(z) - F_{NMID}), \quad \text{with } F_{NMCL}(z) = a + bz \quad \text{and} \quad 0 \leq \lambda \leq 1 \quad (7)$$

$$\dot{m} = -\eta F_N, \quad (8)$$

where eq. (6) is the aerodynamic polar, eq. (7) describes the net thrust, eq. (8) represents the fuel flow,  $\lambda$  is the thrust ratio, and  $C_{x_0}$ ,  $k$ ,  $a$ ,  $b$  and  $\eta$  are given parameters dependent on the aircraft type model and supposed to be constant. In addition, the aircraft performance is limited, and the aircraft trajectory is subject to some Air Traffic Control (ATC)

constraints and structural limitations:

$$\begin{cases} 0 \leq C_z \leq C_{z_{max}} \\ 0 \leq CAS(v, z) \leq VMO \\ 0 \leq M(v, z) \leq MMO \\ F_{NMID} \leq F_N \leq F_{NMCL} \\ V_{z_{min}} \leq v \sin \gamma \leq V_{z_{max}}, \end{cases} \quad (9)$$

where  $CAS$  is the Calibrated AirSpeed,  $M$  represents the Mach number,  $VMO$  is the upper bound on calibrated airSpeed,  $MMO$  is the Maximum Operating Mach number,  $V_{z_{min}}$  and  $V_{z_{max}}$  are the upper and lower bounds of the vertical speed, and  $F_{NMID}$  and  $F_{NMCL}$  are the thrust limits. In our study we consider  $F_{NMID} = 0$ .

## B. Optimal control formulation

A general optimal control problem consists in finding a control vector,  $\mathbf{u}(t)$ , that minimizes some given cost (objective) function,  $J : \mathbb{R}^{n_x} \times \mathbb{R}^{n_u} \times [t_0, t_f] \rightarrow \mathbb{R}$ , presented in a Bolza form in eq. (10):

$$J = \phi_f(\mathbf{x}(t_f), \mathbf{u}(t_f)) + \int_{t_0}^{t_f} \phi_t(\mathbf{x}(t), \mathbf{u}(t), t) dt, \quad (10)$$

where  $\mathbf{x}(t) \in \mathbb{R}^{n_x}$  is the state vector, and  $\mathbf{u}(t) \in \mathbb{R}^{n_u}$  is the control vector which must satisfy, for  $t_0 \leq t \leq t_f$ :

1. the dynamics equations:

$$\dot{\mathbf{x}}(t) = f(\mathbf{x}(t), \mathbf{u}(t), t), \quad (11)$$

2. the initial and terminal conditions at some given times  $t_0$  and  $t_f$ :

$$\mathbf{x}(t_0) = \mathbf{x}_0 \quad (12)$$

$$\mathbf{x}(t_f) = \mathbf{x}_f, \quad (13)$$

3. the algebraic path constraints:

$$\mathbf{g}_l \leq \mathbf{g}(\mathbf{x}(t), \mathbf{u}(t), t) \leq \mathbf{g}_u, \quad (14)$$

4. the bounds on  $\mathbf{x}$  and  $\mathbf{u}$ :

$$\mathbf{x}_l \leq \mathbf{x}(t) \leq \mathbf{x}_u \quad (15)$$

$$\mathbf{u}_l \leq \mathbf{u}(t) \leq \mathbf{u}_u, \quad (16)$$



where the function  $f : \mathbb{R}^{n_x} \times \mathbb{R}^{n_u} \times [t_0, t_f] \rightarrow \mathbb{R}^{n_x}$  is the right-hand side function of the differential-algebraic system (11),  $\mathbf{x}_0 \in \mathbb{R}^{n_x}$  and  $\mathbf{x}_f \in \mathbb{R}^{n_x}$  are respectively the vectors of initial and terminal conditions, the function  $\mathbf{g}(\mathbf{x}(t), \mathbf{u}(t), t)$  represents the set of path constraints with lower bound  $\mathbf{g}_l$  and upper bound  $\mathbf{g}_u$ , and where  $\mathbf{x}_l \in \mathbb{R}^{n_x}$ ,  $\mathbf{x}_u \in \mathbb{R}^{n_x}$  and  $\mathbf{u}_l \in \mathbb{R}^{n_u}$ ,  $\mathbf{u}_u \in \mathbb{R}^{n_u}$  are the lower and upper bounds of the state and control vectors respectively.

In our approach the time,  $t_f$ , at the end of the trajectory is unknown. A commonly-used method to deal with free final-time problems is to rewrite the dynamics equations as functions of an independent variable other than time [58–60]. In consequence, we choose the longitudinal distance,  $s$ , as the evolution variable and the time,  $t$ , becomes a state component. In this paper, the state  $\mathbf{x}$  and control  $\mathbf{u}$  are defined for the whole mission as:

$$\begin{cases} \mathbf{x} = [v, m, z, t] \\ \mathbf{u} = [\gamma, \lambda]. \end{cases} \quad (17)$$

Our aim is to compute a control vector over the distance interval  $[s_0, s_f]$ , that minimizes some cost function subject to constraints that are detailed below. This study focuses on minimizing the fuel burned. This boils down to minimize:

$$J = \int_{s_0}^{s_f} \frac{dm}{ds}(\mathbf{x}, \mathbf{u}, s) ds. \quad (18)$$

In order to guarantee a flyable trajectory, several constraints must be considered, in particular the dynamics of the system (11), which is modeled in Subsection III.A. Thus, based on motion equations (1), (2), (3) and (4) and on the performance equations (6), (7) and (8), the aircraft dynamic model equations read:

$$\begin{cases} \frac{dv}{ds}(\mathbf{x}, \mathbf{u}, s) = \frac{\dot{v}}{\dot{s}} = \frac{F_N}{mv \cos \gamma} - \frac{\frac{1}{2}\rho v S_{ref} C_x(C_z)}{m \cos \gamma} - \frac{g_0}{v} \tan \gamma \\ \frac{dm}{ds}(\mathbf{x}, \mathbf{u}, s) = \frac{\dot{m}}{\dot{s}} = -\frac{\eta F_N}{v \cos \gamma} \\ \frac{dz}{ds}(\mathbf{x}, \mathbf{u}, s) = \frac{\dot{z}}{\dot{s}} = \tan \gamma \\ \frac{dt}{ds}(\mathbf{x}, \mathbf{u}, s) = \frac{1}{\dot{s}} = \frac{1}{v \cos \gamma}, \end{cases} \quad (19)$$

and must be considered as constraints of the problem.

Moreover, the aircraft starts flying from the initial conditions:

$$\begin{cases} v(s_0) = v_0 \\ m(s_0) = m_0 \\ z(s_0) = z_0 \\ t(s_0) = t_0. \end{cases} \quad (20)$$

and reaches the final conditions:

$$\begin{cases} v(s_f) = v_0 \\ z(s_f) = z_0, \end{cases} \quad (21)$$

where the initial longitudinal distance,  $s_0$ , and the final longitudinal distance,  $s_f$ , are given data.

The optimization consists in finding a control vector,  $\mathbf{u}(s)$ , that minimizes the above objective function,  $J$ , while satisfying constraints (19), (20), and (21), as well as the path constraints (9). To summarize, the problem is written as follows:

$$\begin{aligned} \min_{\mathbf{u}} J(\mathbf{x}, \mathbf{u}) &= \int_{s_0}^{s_f} \frac{dm}{ds}(\mathbf{x}, \mathbf{u}, s) ds \\ \text{s.t.} \quad & \begin{cases} \frac{dv}{ds}(\mathbf{x}, \mathbf{u}, s) = \frac{F_N}{mv \cos \gamma} - \frac{\frac{1}{2} \rho v S_{ref} C_x(C_z)}{m \cos \gamma} - \frac{g_0}{v} \tan \gamma \\ \frac{dm}{ds}(\mathbf{x}, \mathbf{u}, s) = -\frac{\eta F_N}{v \cos \gamma} \\ \frac{dz}{ds}(\mathbf{x}, \mathbf{u}, s) = \tan \gamma \\ \frac{dt}{ds}(\mathbf{x}, \mathbf{u}, s) = \frac{1}{v \cos \gamma} \\ 0 \leq C_z \leq C_{z_{max}} \\ 0 \leq CAS(v, z) \leq VMO \\ 0 \leq M(v, z) \leq MMO \\ 0 \leq \lambda \leq 1 \\ V_{z_{min}} \leq v \sin \gamma \leq V_{z_{max}} \\ \mathbf{x}(s_0) = (v_0, m_0, z_0, t_0) \\ v(s_f) = v_0 \\ z(s_f) = z_0. \end{cases} \end{aligned} \quad (22)$$

### C. Optimal control problem resolution methods

Research into the solution of optimal control problems has historically fallen into one of two major categories: indirect methods and direct methods. Indirect methods use the calculus of variations [41, 61] to determine the first-order necessary optimality conditions of the original optimal control problem. They lead to a multiple-point boundary-value

problem. In direct methods, the state and/or control of the optimal control problem is discretized in some manner, and the problem is transcribed [62] into a Nonlinear Programming Optimization problem (NLP). The NLPs produced by direct methods are commonly solved by gradient-based optimization methods, such as sequential quadratic programming [63] or interior point method [64]. In this paper, a direct collocation method and an interior point algorithm are used to solve our problem.

Direct methods are divided into two main classes: direct shooting and direct collocation methods [41, 62]. In the direct shooting method only the control is discretized, whereas the direct collocation deals with the discretization of both the state and control variables. Here, we focus on direct collocation as it is particularly robust for problems with difficult path constraints, and it can be applied without determining or even knowing any necessary optimality conditions as in indirect methods, which can be particularly useful for problems whose adjoint functions are hard to determine [35].

The original infinite and continuous problem is therefore discretized, and transformed into a nonlinear programming (NLP) problem involving a finite set of variables. Several collocation strategies are found in the literature, like for instance Euler, trapezoidal, Runge-Kutta, Hermite-Simpson, pseudo-spectral methods [35, 41, 65, 66]. They only differ in the way they formulate the dynamic constraints. Here, we choose a trapezoidal collocation method as it represents a good trade-off between the accuracy of the produced trajectory and the algorithm execution time [67].

As a first step, the evolution variable interval is divided into a predefined number of segments whose start-end points are called *collocation points*. Then, consider the along-path distance  $s \in [s_0, s_f]$  as the evolution variable, and assume that it is divided into  $N$  segments with:

$$s_0 \leq s_1 \leq \dots \leq s_N = s_f.$$

Next, we need to discretize the trajectory, so as to obtain a finite number of decision variables. In order to do so, we represent the state,  $\mathbf{x}(s)$ , and the control,  $\mathbf{u}(s)$ , by their values  $\mathbf{x}_k$  and  $\mathbf{u}_k$  at each collocation point:

$$\mathbf{x}_k = (x_{1,k}, x_{2,k}, \dots, x_{i,k}, \dots, x_{n_x,k})^\top, \quad k = 0, 1, \dots, N$$

$$\mathbf{u}_k = (u_{1,k}, u_{2,k}, \dots, u_{j,k}, \dots, u_{n_u,k})^\top, \quad k = 0, 1, \dots, N - 1.$$

Then, for  $i = 1, 2, \dots, n_x$  we consider the dynamic system  $\frac{dx_i(s)}{ds} = f_i(\mathbf{x}(s), \mathbf{u}(s), s)$ , where  $x_i$  and  $f_i$  are respectively the  $i^{\text{th}}$  component of the state vector  $\mathbf{x}$  and of the differential-algebraic system (11). We obtain a set of algebraic equations (*collocation constraints*) by integrating both sides of the dynamic system. The integral over each segment  $[s_k, s_{k+1}]$  is numerically approximated via the trapezoidal rule, yielding:

$$x_{i,k+1} - x_{i,k} \approx \frac{1}{2} \tau_k (f_i(\mathbf{x}_{k+1}, \mathbf{u}_k, s_{k+1}) + f_i(\mathbf{x}_k, \mathbf{u}_k, s_k)), \quad k = 0, 1, \dots, N - 1, \quad (23)$$

where  $\tau_k = s_{k+1} - s_k$ . Note that it is the  $k^{th}$  component of the control vector,  $\mathbf{u}$ , that is considered in both terms of the right-hand side part of the transcription equation (23). In addition to this approximation of the dynamic system, constraints (14), (15) and (16) must also be evaluated and enforced at collocation points.

The number of segments,  $N$ , is chosen by the user based on the desired trade-off between desired accuracy and algorithm execution time.

Finally, this discretized NLP problem is solved by an interior point solver.

#### IV. Numerical experiments

The methodology described above is applied to the optimization of twelve missions. These test problems correspond to all combinations of four different ranges (1, 000; 2, 000; 4, 000 and 6, 000 km) and three initial weights\* (60, 77 and 89 metric tons). For instance, a mission of 6, 000 km (3, 240 NM) with 77 tons as initial weight will be referred to as 77t/6000km.

The performance parameters used in all these case studies are described in Table 1. The mission length,  $s_f$ , is discretized into  $N = 500$  collocation points. Table 2 displays the initial and final conditions. The computation is performed on a workstation equipped with an Intel Core i7 CPU running at 2.71 GHz.

**Table 1 Performance parameters.**

Performance parameter	Description	Value
$\eta$	Specific consumption	$1.5110^{-5}$ kg/N.s
a	MCL net thrust at sea level	141, 000 N
b	MCL net thrust dependency with altitude	-2.45 N/ft
$C_{x0}$	Parasitic drag coefficient	0.028
$k$	Induced drag coefficient	0.027
S	Aerodynamic reference surface	120 m <sup>2</sup>
<i>VMO</i>	Maximum CAS	180.06 m/s (350 kt)
<i>MMO</i>	Maximum Mach	0.85
$V_{zmin}$	Minimum vertical speed	-3, 000 ft/min
$V_{zmax}$	Maximum vertical speed	3, 000 ft/min
$C_{zmax}$	Maximum lift coefficient	1

To make the search for an optimal trajectory more efficient, it is crucial to provide a feasible and realistic initial guess for the optimization algorithm. To achieve this, the initial-guess trajectory is generated using an Airbus proprietary tool for aircraft trajectory planning. This starting solution includes a climb phase, followed by a single cruise phase at a *non-optimized* constant altitude, and a continuous descent phase for each case study. The tool utilizes performance and integration models that differ from the simplified ones outlined in Subsections III.A and III.C. To ensure the feasibility of the initial solution, an integration process based on our dynamic model and on the trapezoidal rule is used to find

\*As it is common practice in aeronautics, we shall use *weight* for *mass*

**Table 2 Initial conditions and terminal conditions.**

Description	Value
$z_0$	3,048 m (10,000 ft)
$v_0$ (TAS)	148.16 m/s (250 kt CAS at 10,000 ft)
$m_0$	60 t/77 t/89 t
$t_0$	0 s
$s_0$	0 m
$z_f$	3,048 m (10,000 ft)
$v_f$ (TAS)	148.16 m/s (250 kt CAS at 10,000 ft)
$s_f$	1,000 km/2,000 km/4,000 km/6,000 km

the control vector associated with the state vector of the Airbus trajectory. This new initial guess greatly improves convergence and reduces the computation time of the optimization algorithm. We insist on the fact that the Airbus' tool trajectory is not optimized: it is solely used to provide an initial feasible solution.

The previously-described trajectory optimization problem is implemented using CasADi [68] interface in Python, and our resulting NLPs are solved by the interior point optimization solver Ipopt [64]. For  $N = 500$  collocation points, our methodology requires around 10 seconds for each case study.

Subsection IV.A presents a classical result of the mission optimization leading to a continuous ascendant cruise (climb cruise). On the one hand, the obtained results show that our proposed method is viable. On the other hand, these optimal trajectories will be used as good and feasible initial solutions in the sequel. Subsection IV.B proposes a penalty strategy to make the computed mission compliant with current ATM regulations.

### A. Cruise climb

The twelve case studies produce similar vertical profiles. More precisely, they all feature a continuous ascent cruise phase exhibiting a small vertical speed. The case study 77t/6000km will be used for illustration in the following.

The resulting optimal trajectory of the 77t/6000km case study is presented by a solid line in Figure 2 together with the initial-guess trajectory (dashed line). This optimal solution features the well-known ideal cruise vertical profile called *cruise climb*. This is consistent with results found in the literature [54], and can be roughly explained as follows. Suppose that the aircraft is balanced, and is flying with the most efficient thrust settings. The fuel consumption makes the weight decreases, so the lift required to ensure vertical balance also decreases. As a consequence, the corresponding drag decreases, and therefore the required thrust to ensure the propulsive balance is lowered. Nevertheless, instead of reducing the throttle, the best solution is to sustain the efficient setting and to use the thrust excess to climb, slowly.

The optimum vertical speed profile is displayed in Figure 3 where the vertical speed is maintained at a small positive value (9 ft/min) during the cruise climb (see Figure 4), and the horizontal lines represent the vertical air speed bounds. The excess of thrust (or kinetic energy) at the end of the cruise is reflected by a sudden altitude increase (change) to

dissipate this surplus and to reduce the speed needed for descent.

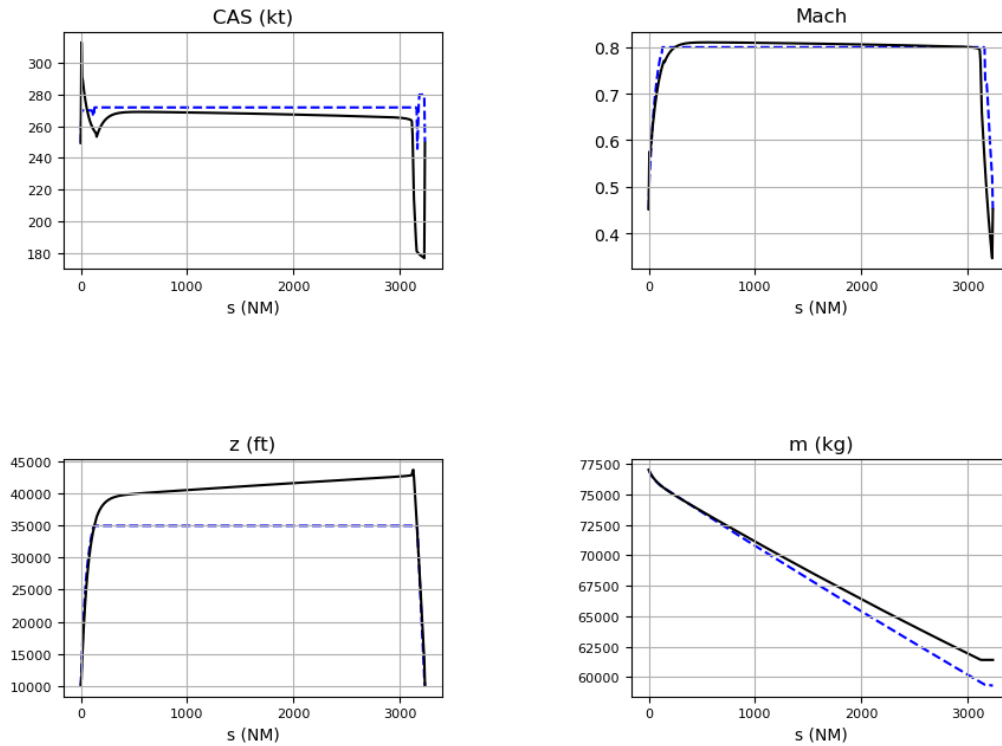


**Fig. 2 Initial guess (dashed line) and optimal trajectory (solid line) with a cruise climb.**

A fuel saving of around 2,100 kg compared to the consumption of the initial-guess trajectory can be observed in Figure 2 (bottom, right). This value is high because the initial trajectory is far from being optimal. This mainly shows that the fuel consumption strongly depends on the trajectory, and motivates the need of its optimization. For the other case studies, the resulting optimal trajectories show similar cruise climb profile. Note that we observe that any feasible, and not necessary optimal, initial trajectory with flight levels also leads to an optimal cruise climb trajectory.

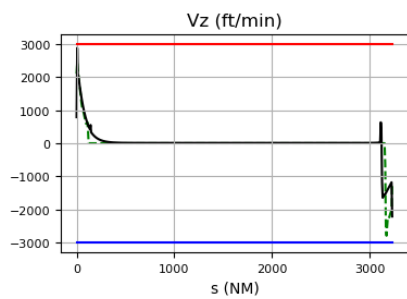


**Fig. 3 Optimal vertical speed profile.**

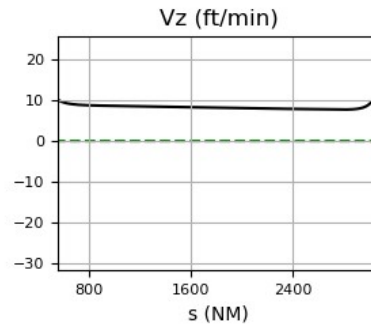


**Fig. 4 Optimal vertical speed in cruise.**

Continuous operations comprising an uninterrupted climb undoubtedly provide the best possible savings in term of

fuel, but the implementation of these operations involves several issues. On the one hand, the prescribed vertical speed is too small to be accurately operated by pilots, or even by autopilots. On the other hand, current air traffic regulations do not allow aircraft to follow such an optimal cruise (continuous) climb profile. The next section proposes a solution to address these issues.

## B. Sinusoidal penalty for cruise levels

In the current *Concept of Operations* (ConOps), aircraft are required to fly at (piecewise) constant cruise altitudes with short climb/descent segments when changing levels. This rule ensures vertical separation of aircraft and makes easier the assurance of safe separation by air traffic control. To enforce cruising levels in our trajectory optimization problem, a penalization approach is proposed. It penalizes the objective function when level flight is not maintained.

We propose a penalty function to model the requirement that the cruise altitude,  $z$ , must take discrete values that are multiples of  $\Delta z_{FL} = 2,000$  ft intervals. This penalty function, inspired by the sine function introduced in [69], is defined as:

$$\frac{1 - \cos\left(\frac{2\pi}{\Delta z_{FL}}z\right)}{2}.$$

We activate it only when the altitude,  $z$ , is above a given threshold height,  $p$ , by using a sigmoid function,  $\phi_p$ , that progressively introduces the penalty. Hence, our penalty function,  $\Psi(z)$ , has the form:

$$\Psi(z) = \phi_p(z) \cdot \frac{1 - \cos\left(\frac{2\pi}{\Delta z_{FL}}z\right)}{2}.$$

This penalty term is multiplied by a user-defined weighting coefficient  $\mu > 0$ , and added to the objective function (18). The penalty parameter,  $\mu$ , controls the relative importance of the penalty term. The value of  $\mu$  is set through an empirical study which shows that the results remain stagnant above a certain threshold value (we use in our tests  $\mu_0 = 0.1$ ). The new objective function becomes:

$$J_\mu(\mathbf{x}, \mathbf{u}) = \int_{s_0}^{s_f} \frac{dm}{ds}(\mathbf{x}, \mathbf{u}, s) ds + \mu \cdot \Psi(z).$$

The tests performed on this penalized objective function lead, here again, to results that are similar for the twelve case studies: flight levels in the cruise phase emerge naturally. For illustration, the resulting optimal trajectory of the 77t/6000km case is detailed. In order not to bias the solver for the optimal cruise levels, we choose the solution of the ascendant cruise problem as initial-guess, rather than the Airbus internal tool solution that already contains level flights. Remark that the initial guess is post-treated in order to remove the artificial peak (at the end of the cruise phase) that was observed above in Figure 2. Results corresponding to the 77t/6000km case study are presented in Figure 5, where the solid line shows the optimal trajectory obtained when considering the penalty term, and the dashed line represents the

initial-guess trajectory (the ascendant cruise solution). As expected, flight levels appear and match rather well the ideal cruise climb trajectory. Perturbations of *CAS* and vertical speed are observed at the end of the climb phase in Figures 5 and 6, and are mostly due to small step climbs.

This penalization approach allows one to find the cruise levels that match the ideal cruise altitude profile at the expense of only a low degradation (62 kg) of the fuel consumption. A low degradation is also noticed for the eleven other missions as illustrated in Figure 7.

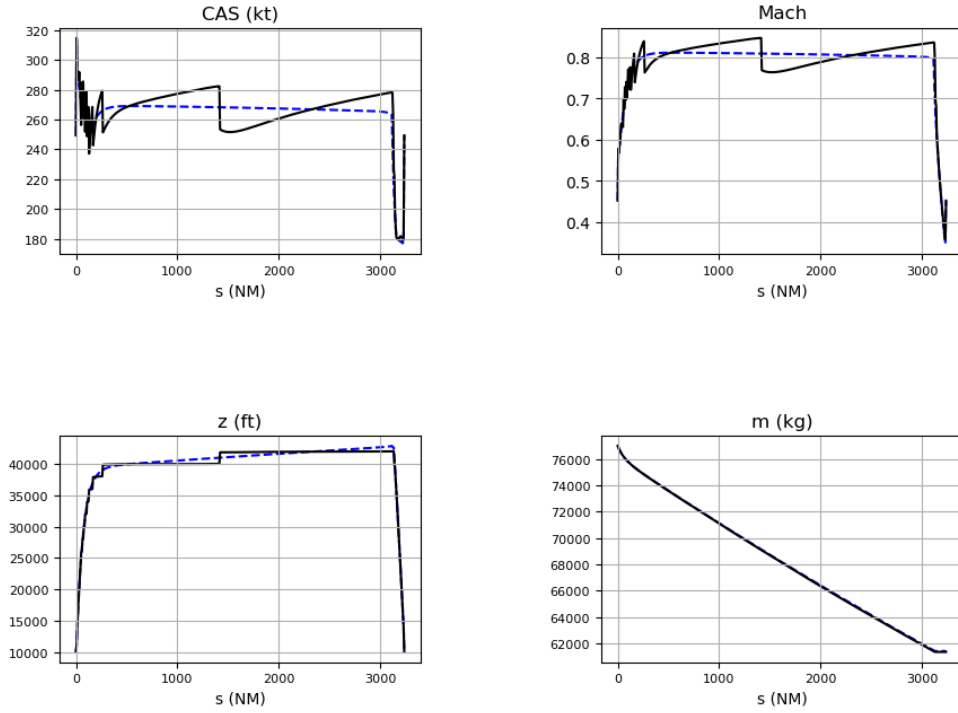


**Fig. 5 Optimal trajectory with the penalty approach.**

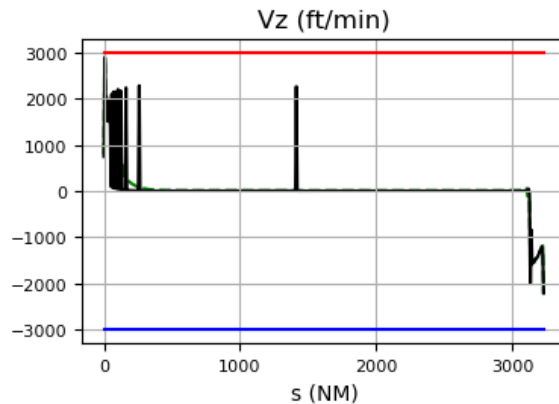


**Fig. 6 Optimal vertical speed with the penalty approach.**



The range has a first-order impact on the degradation of the gain obtained with the ascendant cruise. This degradation is more important for higher ranges, due to longer durations in non-optimal altitudes during the cruise phase. The initial weight has only a small impact on the consumption degradation. Indeed, one observes that the flight levels match well the ideal cruise which represents the optimal altitude for each initial weight. For all twelve cases, enforcing operational flight levels has a negligible impact on the fuel consumption: the relative consumption degradation (ratio between the fuel consumption reduction compared to the cruise climb results and the initial mass for each case study) remains always lower than 1%.

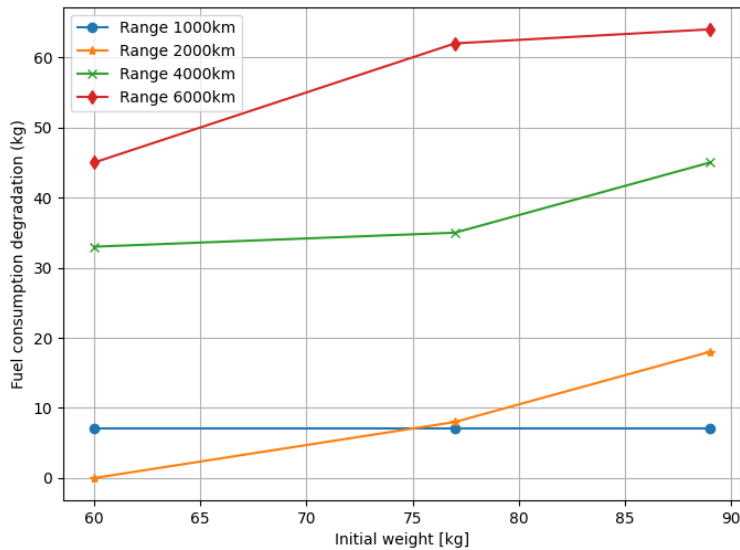


**Fig. 7 Fuel consumption degradation.**

Our penalty approach leads to the natural emergence of cruise levels at the expense of only a negligible overconsumption compared to the optimal ascending cruise solutions. However, too short cruise level segments appear, generally at the end of the initial climb (see Figure 5), and these are not operationally acceptable. This behavior could be addressed in future work by attempting to limit the minimum duration of flight levels.

## V. Multi-start heuristic

Our penalty approach makes the problem strongly non-convex, due to the sinusoidal function that induces several locally-optimal solutions. Therefore, descent methods used by solvers such as Ipopt are likely to converge towards local minima. A simple way to address this issue is to use various starting points in order to explore more widely the search space, increasing thereby the probability of finding a globally-optimal (or at least a good) solution.

Such a multi-start heuristic requires the user to generate several initial solutions that are feasible, because starting

Ipopt with non-feasible solutions yields convergence times that may be unacceptable for operational purposes. Natural feasible initial solutions are trajectories involving one-level cruise at different altitudes. However, tests show that the resulting solutions then do not escape the flight level corresponding to these initial solutions given as input. An

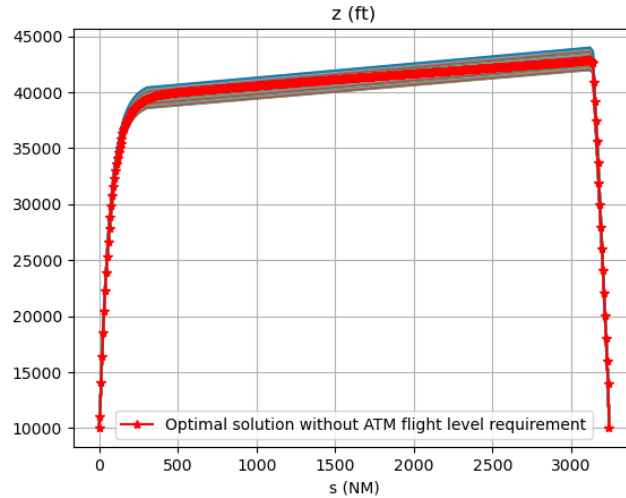


**Fig. 8 Ascendant cruise initial solutions**

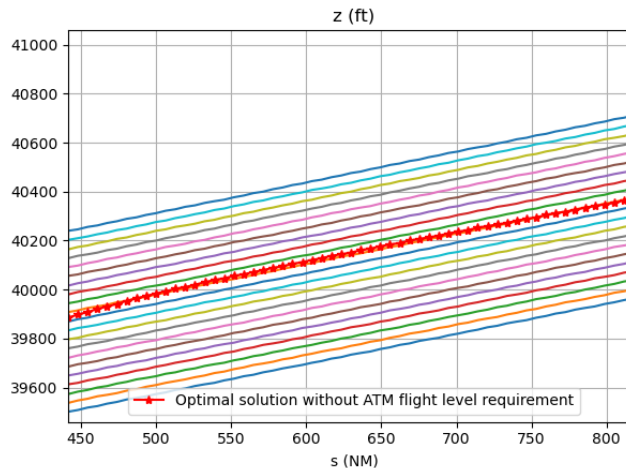


**Fig. 9 Zoom on the ascendant cruise in Figure 8**

alternative natural idea, avoiding this drawback, consists in generating additional continuous-climb trajectories by simply translating the ascending part of the optimal solution obtained with our methodology without the ATM flight-level requirement (see Subsection IV.A, Figure 8, and Figure 9). Each such feasible solution has the advantage of going through several flight levels, and does not bias the solver towards predetermined flight levels.

As a first test, we launch our algorithm with 500 different initial solutions for the mission 77t/6000km. These initial trajectories are labeled from 1 to 500, starting from the lowest cruise altitudes to the highest ones. The initial

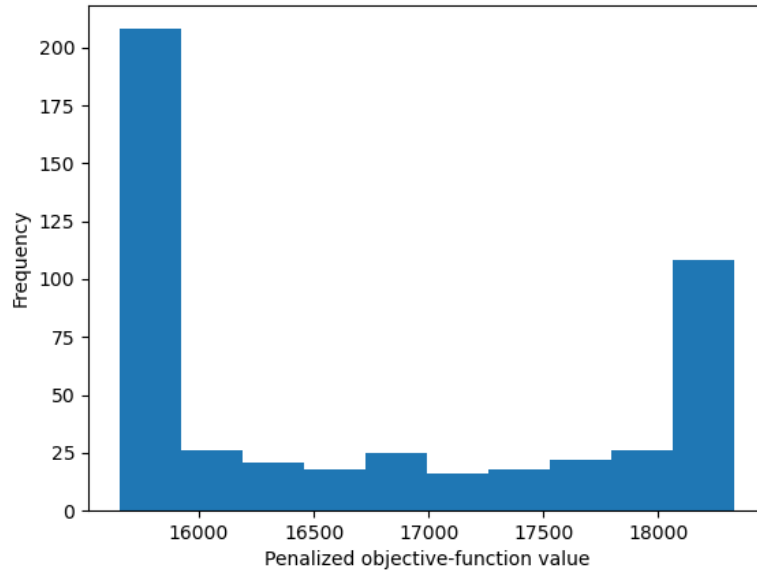


**Fig. 10 Multi-start minimal solution distribution**

solutions that are near the optimal ascendant cruise obtained in Subsection IV.A lead to optimal trajectories featuring the best objective-function values (yellow squares in Figure 12).

Half of the optimal solutions obtained are close to the best one, and feature the same value of the penalized objective function,  $J_\mu$ , (see Figures 10 and 11). Moreover, the histogram of Figure 10 shows that the *basin of attraction* of the global-minimum value is quite large, so there is no need to launch the multi-start heuristic with so many initial solutions. Therefore, in the sequel we are content with initializing our algorithm with only the 20 initial solutions that are closest to the optimal ascendant cruise (see Figure 8). The results show that a very simple multi-start heuristic with only 20 initial solutions is satisfying as most of these 20 initial guesses lead mostly to the same (probably globally-optimal) solution (Figure 13). One moreover observes that the 20 trajectories obtained have identical cruise flight levels; there are only slight variations in the position at which there is a flight-level change, but this does not significantly impact fuel consumption. The curves representing the optimal-weight evolutions appear to be merged on Figure 13 because they are almost identical.

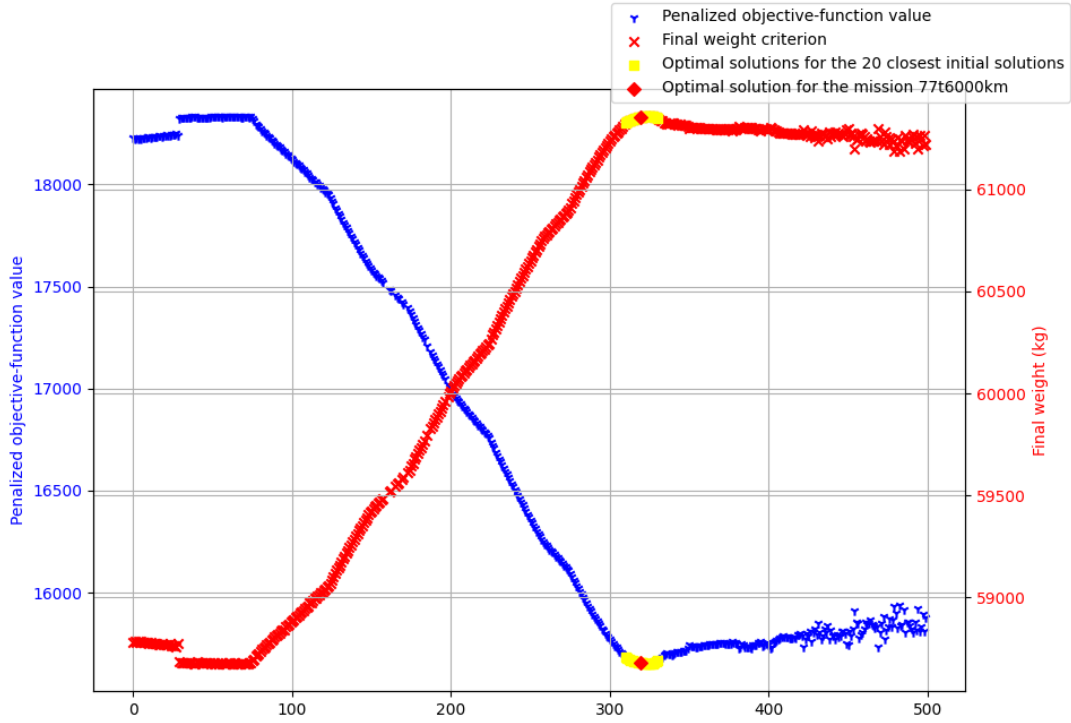


**Fig. 11 Multi-start results for the 77t/6000km mission (500 initial solutions)**

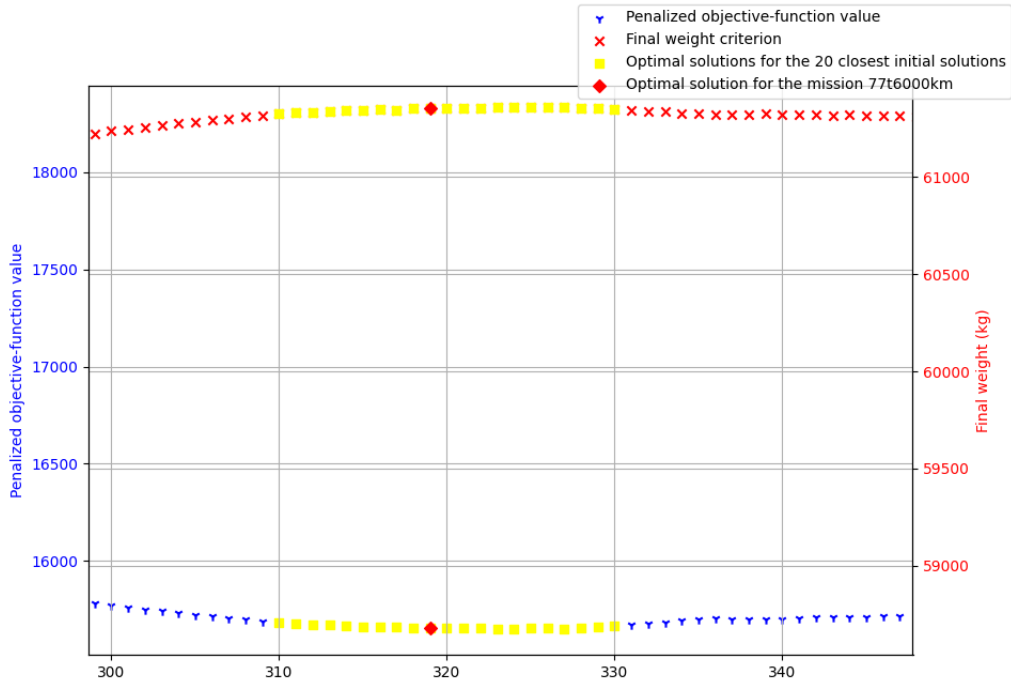


**Fig. 12 Zoom on the optimal solutions corresponding to the 20 closest initial solutions**

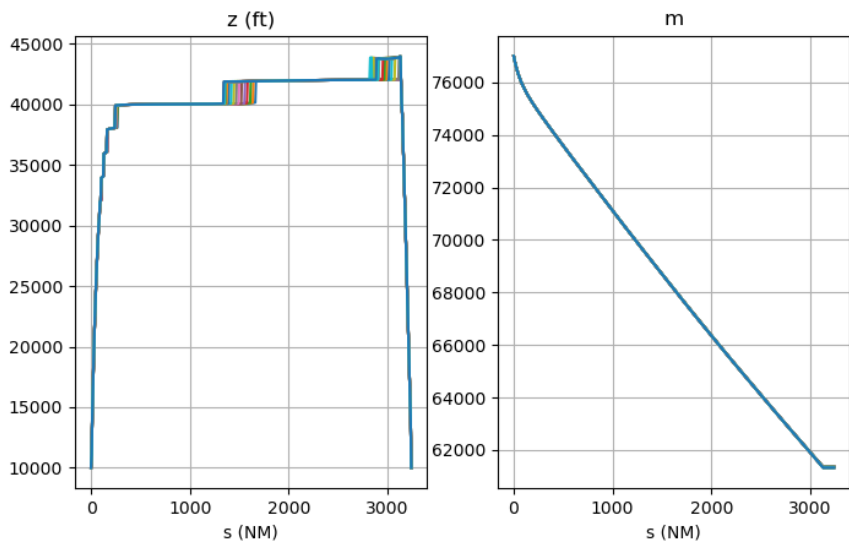


**Fig. 13 The 20 optimal vertical profiles and weight evolutions obtained from the 20 initial solutions**

## VI. Perspectives and conclusions

The preliminary results presented in this article show the proof of concepts of our trajectory optimization approach. We have demonstrated that one can optimize a complete vertical profile without imposing *a priori* its structure in the different phases. Our unified formulation describes the dynamics of the aircraft with a single set of equations which is common to all phases (climb, cruise and descent), and does not need to impose beforehand the number of cruise flight levels. The optimization problem is formulated as an optimal control problem that is transcribed by a classical direct collocation technique, and solved with the python-based CasADi library for NLP modeling and the interior point NLP solver Ipopt.

Our results lead to ATC-compliant trajectories at the expense of a moderate degradation of the fuel consumption, compared to the ideal solution with the ascendant cruise. Another contribution of our approach is the “natural” emergence of cruise flight levels in the solution. Finally, preliminary results indicate that a simple multi-start heuristic is sufficient to find globally-optimal solutions for the penalized problem.

Our research work opens up several avenues for future work. The first one is to conduct extensive numerical experiments on more cases, with a sensitivity analysis on the parameters defining them. A second track of research is to take wind into account. A third challenging issue is to combine our approach with lateral profile optimization. These perspectives pave the way for the development of a more operational approach that can be used by airlines.

## Acknowledgements

The first author’s PhD was financially supported by Airbus and ANRT.

## References

- [1] Lee, D. S., Fahey, D. W., Forster, P. M., Newton, P. J., Wit, R. C., Lim, L. L., Owen, B., and Sausen, R., “Aviation and global climate change in the 21st century,” *Atmospheric Environment*, Vol. 43, No. 22-23, 2009, pp. 3520–3537. <https://doi.org/https://doi.org/10.1016/j.atmosenv.2009.04.024>
- [2] Hartjes, S., Hendriks, T., and Visser, D., “Contrail mitigation through 3D aircraft trajectory optimization,” *16th AIAA Aviation Technology, Integration, and Operations Conference*, 2016, pp. 13–17. <https://doi.org/https://doi.org/10.2514/6.2016-3908>
- [3] Penner, J. E., Lister, D., Griggs, D., and MacFarland, D. D. M., *Aviation and the global atmosphere, intergovernmental panel on climate change special report*, Cambridge University Press, Cambridge, UK, 1999.
- [4] Zhang, M., Filippone, A., and Bojdo, N., “Using trajectory optimization to minimize aircraft noise impact,” *INTER-NOISE and NOISE-CON Congress and Conference Proceedings*, Vol. 255, Institute of Noise Control Engineering, 2017, pp. 4003–4013.
- [5] Ky, P., and Miaillier, B., “SESAR : Towards the new generation of air traffic management systems in Europe,” *The Journal of Air Traffic Control*, Vol. 48, 2006.
- [6] “NextGen implementation plan,” , 2013. Federal Aviation Administration, Washington DC, USA.
- [7] Gardi, A., Sabatini, R., and Trevor, K., “Multiobjective 4D trajectory optimization for integrated avionics and air traffic management systems,” *IEEE Transactions on Aerospace and Electronic Systems*, Vol. 55, No. 1, 2019, pp. 170–181. <https://doi.org/10.1109/TAES.2018.2849238>.
- [8] Kasturi, E., Devi, S. P., Kiran, S. V., and Manivannan, S., “Airline route profitability analysis and optimization using BIG DATA analytics on aviation data sets under heuristic techniques,” *Procedia Computer Science*, Vol. 87, 2016, pp. 86 – 92. <https://doi.org/10.1016/j.procs.2016.05.131>.
- [9] Koksalmis, G., “Operations management perspectives in the air transport management,” *Journal of Business Administration Research*, Vol. 2, No. 1, 2019. <https://doi.org/10.30564/jbar.v2i1.288>.
- [10] Khardi, S., “Development of innovative optimized flight paths of aircraft takeoffs reducing noise and fuel consumption,” *Acta Acustica united with Acustica*, Vol. 97, 2011, pp. 148–154. <https://doi.org/10.3813/AAA.918395>.
- [11] Cots, O., Gergaud, J., and Goubinat, D., “The minimum time-to-climb and fuel consumption problems and CAS/Mach procedure for aircraft,” 2018. URL <https://hal.archives-ouvertes.fr/hal-01936193/document>.
- [12] Wu, D., and Zhao, Y., “Optimization and sensitivity analysis of climb and descent trajectories for reducing fuel burn and emissions,” *11th AIAA Aviation Technology, Integration, and Operations (ATIO) Conference, including the AIAA Balloon Systems Conference and 19th AIAA Lighter-Than, Air Technology Conference*, 2011, pp. 6879–6902. <https://doi.org/https://doi.org/10.2514/6.2011-6879>
- [13] Antoine, N. E., and Kroo, I. M., “Framework for aircraft conceptual design and environmental performance studies,” *AIAA Journal*, Vol. 43, No. 10, 2005, pp. 2100–2109. <https://doi.org/10.2514/1.13017>.

- [14] Andreu Altava, R., Mere, J. C., Delahaye, D., and Miquel, T., “Graph-search descent and approach trajectory optimization based on enhanced aircraft energy management,” *AIAA Aviation 2019 Forum*, 2019, p. 3618. <https://doi.org/https://doi.org/10.2514/6.2019-3618>
- [15] Dalmau, R., Prats, X., Verhoeven, R., Bussink, F., and Heesbeen, B., “Comparison of various guidance strategies to achieve time constraints in optimal descents,” *Journal of Guidance, Control, and Dynamics*, Vol. 42, No. 7, 2019, pp. 1612–1621. <https://doi.org/https://doi.org/10.2514/1.G004019>
- [16] Park, S. G., and Clarke, J. P., “Vertical trajectory optimization for continuous descent arrival procedure,” *AIAA Guidance, Navigation, and Control Conference*, 2012, p. 4757. <https://doi.org/https://doi.org/10.2514/6.2012-4757>
- [17] Park, S. G., and Clarke, J. P., “Vertical trajectory optimization to minimize environmental impact in the presence of wind,” *Journal of Aircraft*, Vol. 53, No. 3, 2016, pp. 725–737. <https://doi.org/10.2514/1.C032974>.
- [18] Nikoleris, T., Chatterji, G. B., and Coppenbarger, R. A., “Comparison of fuel consumption of descent trajectories under arrival metering,” *Journal of Aircraft*, Vol. 53, No. 6, 2016, pp. 1853–1864. <https://doi.org/https://doi.org/10.2514/1.C033374>.
- [19] Pawełek, A., Lichota, P., Dalmau, R., and Prats, X., “Fuel-efficient trajectories traffic synchronization,” *Journal of Aircraft*, Vol. 56, No. 2, 2019, pp. 481–492. <https://doi.org/10.2514/1.C034730>.
- [20] Andreu Altava, R., Mere, J. C., Neri, P., Delahaye, D., and Miquel, T., “Flight simulator evaluation of fuel-efficient arrival profiles,” *Journal of Guidance, Control, and Dynamics*, Vol. 43, No. 11, 2020, pp. 2165–2174. <https://doi.org/https://doi.org/10.2514/1.G005091>
- [21] Altava, R. A., Mere, J. C., Neri, P., Delahaye, D., and Miquel, T., “Raising flight crew aircraft energy awareness through high-energy-limit trajectories,” *Journal of Aircraft*, Vol. 57, No. 5, 2020, pp. 817–829. <https://doi.org/10.2514/1.C035934>.
- [22] Khardi, S., and Abdallah, L., “Optimization approaches of aircraft flight path reducing noise: Comparison of modeling methods,” *Applied Acoustics*, Vol. 73, No. 4, 2012, pp. 291–301. <https://doi.org/10.1016/j.apacoust.2011.06.012>.
- [23] Betts, J. T., and Cramer, E. J., “Application of direct transcription to commercial aircraft trajectory optimization,” *Journal of Guidance, Control, and Dynamics*, Vol. 18, No. 1, 1995, pp. 151–159. <https://doi.org/10.2514/3.56670>.
- [24] Norsell, M., “Multistage trajectory optimization with radar range constraints,” *Journal of Aircraft*, Vol. 42, No. 4, 2005, pp. 849–857. <https://doi.org/https://doi.org/10.2514/1.8544>
- [25] Ringertz, U., “Aircraft trajectory optimization as a wireless internet application,” *Journal of Aerospace Computing Information and Communication*, Vol. 1, 2004, pp. 85–99. <https://doi.org/10.2514/1.1279>.
- [26] Soler, M., Olivares, A., and Staffetti, E., “Framework for aircraft trajectory planning toward an efficient air traffic management,” *Journal of Aircraft*, Vol. 49, 2012, pp. 341–348. <https://doi.org/10.2514/1.C031490>.
- [27] Vilardaga, S., Prats, X., Duan, P. P., and Uijt de Haag, M., “Conflict-free trajectory optimization with target tracking and conformance monitoring,” *Journal of Aircraft*, Vol. 55, No. 3, 2018, pp. 1252–1260. <https://doi.org/10.2514/1.C034251>.

- [28] Hedrick, J. K., and Bryson, A. E., “Three-dimensional minimum-time turns for a supersonic aircraft,” *Journal of Aircraft*, Vol. 9, No. 2, 1972, pp. 115–121. <https://doi.org/10.2514/3.58943>.
- [29] Barman, J. F., and Erzberger, H., “Fixed-range optimum trajectories for short-haul aircraft,” *NASA TN D-8115, Ames research center, Moffett Field, CA, USA*, 1975.
- [30] Barman, J. F., and Erzberger, H., “Fixed-range optimum trajectories for short-haul aircraft,” *Journal of Aircraft*, Vol. 13, No. 10, 1976, pp. 748–754. <https://doi.org/10.2514/3.58706>.
- [31] Erzberger, H., and Lee, H., “Constrained optimum trajectories with specified range,” *Journal of Guidance and Control*, Vol. 3, No. 1, 1980, pp. 78–85. <https://doi.org/10.2514/3.55950>.
- [32] Sorensen, J. A., Morello, S. A., and Erzberger, H., “Application of trajectory optimization principles to minimize aircraft operating costs,” *1979 18th IEEE Conference on Decision and Control including the Symposium on Adaptive Processes*, Vol. 2, 1979, pp. 415–421. <https://doi.org/10.1109/CDC.1979.270208>
- [33] Visser, H. G., Kelley, H. J., and Cliff, E. M., “Energy management of three-dimensional minimum-time intercept,” *Journal of Guidance, Control, and Dynamics*, Vol. 10, No. 6, 1987, pp. 574–580. <https://doi.org/10.2514/3.20258>.
- [34] Hagelauer, P., and Mora-Camino, F., “A soft dynamic programming approach for on-line aircraft 4D-trajectory optimization,” *European Journal of Operational Research*, Vol. 107, No. 1, 1998, pp. 87–95. [https://doi.org/https://doi.org/10.1016/S0377-2217\(97\)00221-X](https://doi.org/https://doi.org/10.1016/S0377-2217(97)00221-X)
- [35] Betts, J. T., “Survey of numerical methods for trajectory optimization,” *Journal of Guidance, Control, and Dynamics*, Vol. 21, No. 2, 1998, pp. 193–207. <https://doi.org/10.2514/2.4231>.
- [36] Delahaye, D., Puechmorel, S., Tsiotras, P., and Féron, E., “Mathematical models for aircraft trajectory design: A survey,” *Air Traffic Management and Systems*, Springer, 2014, pp. 205–247. [https://doi.org/10.1007/978-4-431-54475-3\\_12](https://doi.org/10.1007/978-4-431-54475-3_12)
- [37] Gardi, A., Sabatini, R., and Ramasamy, S., “Multi-objective optimisation of aircraft flight trajectories in the ATM and avionics context,” *Progress in Aerospace Sciences*, Vol. 83, 2016, pp. 1–36. <https://doi.org/https://doi.org/10.1016/j.paerosci.2015.11.006>
- [38] Hargraves, C. R., and Paris, S. W., “Direct trajectory optimization using nonlinear programming and collocation,” *Journal of Guidance, Control, and Dynamics*, Vol. 10, No. 4, 1987, pp. 338–342. <https://doi.org/https://doi.org/10.2514/6.1986-2000>
- [39] Visser, H. G., “A 4-D trajectory optimization and guidance technique for terminal area traffic management,” *Delft University of Technology, Faculty of Aerospace Engineering, Netherlands, Report LR-769*, 1994.
- [40] Betts, J. T., and Huffman, W. P., “Application of sparse nonlinear programming to trajectory optimization,” *Journal of Guidance, Control, and Dynamics*, Vol. 15, No. 1, 1992, pp. 198–206. <https://doi.org/https://doi.org/10.2514/3.20819>
- [41] Betts, J. T., Bauer, T., Huffman, W., and Zondervan, K., “Solving the optimal control problem using a nonlinear programming technique. I - General formulation,” *Astrodynamics Conference*, 1984, pp. 84–2037. <https://doi.org/https://doi.org/10.2514/6.1984-2037>



- [42] Kirk, D. E., *Optimal control theory: An introduction*, Courier Corporation, 2004.
- [43] Villarroel, J., and Rodrigues, L., “An optimal control framework for the climb and descent economy modes of flight management systems,” *IEEE Transactions on Aerospace and Electronic Systems*, Vol. 52, No. 3, 2016, pp. 1227–1240. <https://doi.org/10.1109/TAES.2016.150135>.
- [44] Soler, M., Alberto, O., and Erbesto, S., “Hybrid optimal control approach to commercial aircraft trajectory planning,” *Journal of Guidance, Control and Dynamics*, Vol. 33, 2010, pp. 385–991. <https://doi.org/https://doi.org/10.2514/1.47458>
- [45] Soler, M., Alberto, O., Erbesto, S., and Pierre, B., “En-route optimal flight planning constrained to pass through waypoints using MINLP,” *Proceedings of 9th USA/Europe Air Traffic Management Research and Development Seminar (ATM 2011)*, 2011.
- [46] González-Arribas, D., Soler, M., Sanjurjo-Rivo, M., Kamgarpour, M., and Simarro, J., “Robust aircraft trajectory planning under uncertain convective environments with optimal control and rapidly developing thunderstorms,” *Aerospace Science and Technology*, Vol. 89, 2019, pp. 445–459. <https://doi.org/https://doi.org/10.1016/j.ast.2019.03.051>
- [47] González-Arribas, D., Soler, M., Sanjurjo-Rivo, M., García-Heras, J., Sacher, D., Gelhardt, U., Lang, J., Hauf, T., and Simarro, J., “Robust optimal trajectory planning under uncertain winds and convective risk,” *ENRI International Workshop on ATM/CNS*, Springer, 2017, pp. 82–103. [https://doi.org/10.1007/978-981-13-7086-1\\_6](https://doi.org/10.1007/978-981-13-7086-1_6)
- [48] González-Arribas, D., Hentzen, D., Sanjurjo-Rivo, M., Soler, M., and Kamgarpour, M., “Optimal aircraft trajectory planning in the presence of stochastic convective weather cells,” *17th AIAA Aviation Technology, Integration, and Operations Conference 2017: Denver, Colorado, USA*, Curran Associates Inc., 2017, p. 3431. <https://doi.org/10.2514/6.2017-3431>.
- [49] González-Arribas, D., Soler, M., and Sanjurjo-Rivo, M., “Robust aircraft trajectory planning under wind uncertainty using optimal control,” *Journal of Guidance, Control, and Dynamics*, Vol. 41, No. 3, 2018, pp. 673–688. <https://doi.org/10.2514/1.G002928>.
- [50] Merrer., M. L., “Optimisation de trajectoire d’avion pour la prise en compte du bruit dans la gestion du vol,” Ph.D. thesis, Université Toulouse 3-Paul Sabatier, France, 2012.
- [51] Eele, A., and Richards, A., “Path-planning with avoidance using nonlinear branch-and-bound optimization,” *Journal of Guidance, Control, and Dynamics*, Vol. 32, No. 2, 2009, pp. 384–394. <https://doi.org/https://doi.org/10.2514/1.40034>
- [52] Bower, G., and Kroo, I., “Multi-objective aircraft optimization for minimum cost and emissions over specific route networks,” *The 26th Congress of ICAS and 8th AIAA ATIO*, 2008, pp. 14–19. <https://doi.org/https://doi.org/10.2514/6.2008-8905>
- [53] Girardet, B., Lapasset, L., Delahaye, D., and Rabut, C., “Wind-optimal path planning: Application to aircraft trajectories,” *13th International Conference on Control Automation Robotics & Vision (ICARCV)*, IEEE, 2014, pp. 1403–1408. <https://doi.org/10.1109/ICARCV.2014.7064521>
- [54] Lovegren, J., and Hansman, R. J., “Estimation of potential aircraft fuel burn reduction in cruise via speed and altitude optimization strategies,” Tech. rep., 2011. Master of Science in Aeronautics and Astronautics, Massachusetts Institute of Technology, Cambridge, MA.

- [55] Dalmau-Codina, R., and Prats, X., “Fuel and time savings by flying continuous cruise climbs,” *Transportation Research Part D: Transport and Environment*, Vol. 35, 2015, pp. 62–71. <https://doi.org/10.1016/j.trd.2014.11.019>.
- [56] Airbus, “Getting to grips with aircraft performance monitoring,” Tech. rep., Airbus, Blagnac, France, 2002. <https://www.skybrary.aero/bookshelf/books/2263.pdf>.
- [57] EUROCONTROL, “User Manual for the Base of Aircraft Data (BADA),” , 2018.
- [58] Lu, P., “Entry guidance: A unified method,” *Journal of Guidance, Control, and Dynamics*, Vol. 37, No. 3, 2014, pp. 713–728. <https://doi.org/10.2514/1.62605>.
- [59] Liu, X., Shen, Z., and Lu, P., “Closed-loop optimization of guidance gain for constrained impact,” *Journal of Guidance, Control, and Dynamics*, Vol. 40, No. 2, 2017, pp. 453–460. <https://doi.org/10.2514/1.G000323>.
- [60] Hong, H., Piprek, P., Gerdt, M., and Holzapfel, F., “Computationally efficient trajectory generation for smooth aircraft flight level changes,” *Journal of Guidance, Control, and Dynamics*, Vol. 44, No. 8, 2021, pp. 1532–1540. <https://doi.org/10.2514/1.G005529>.
- [61] Ascher, U. M., Mattheij, R. M., and Russell, R. D., “Numerical solution of boundary value problems for ordinary differential equations,” *Society for Industrial and Applied Mathematics.*, Vol. 13, 1995. <https://doi.org/https://doi.org/10.1137/1.9781611971231>
- [62] Kraft, D., “On converting optimal control problems into nonlinear programming problems,” *Computational Mathematical Programming*, edited by K. Schittkowski, 1985, pp. 261–280. [https://doi.org/10.1007/978-3-642-82450-0\\_9](https://doi.org/10.1007/978-3-642-82450-0_9)
- [63] Gill, P., Murray, W., and Saunders, M., “SNOPT: An SQP Algorithm for large-scale constrained optimization,” *SIAM Journal on Optimization*, Vol. 12, 2002, pp. 979–1006. <https://doi.org/10.2307/20453604>.
- [64] Wächter, A., and Biegler, L. T., “On the implementation of an interior-point filter line-search algorithm for large-scale nonlinear programming,” *Mathematical Programming*, Vol. 106, No. 1, 2006, pp. 25–57. <https://doi.org/https://doi.org/10.1007/s10107-004-0559-y>
- [65] Becerra, V. M., “Practical direct collocation methods for computational optimal control,” *Modeling and Optimization in Space Engineering*, edited by G. Fasano and J. D. Pintér, Springer, 2012, pp. 33–60. [https://doi.org/10.1007/978-1-4614-4469-5\\_2](https://doi.org/10.1007/978-1-4614-4469-5_2)
- [66] Soler, M., “Commercial aircraft trajectory planning based on multiphase mixed-integer optimal control,” Ph.D. thesis, Universidad Carlos III de Madrid, Spain, 2013.
- [67] Kelly, M., “An introduction to trajectory optimization: How to do your own direct collocation,” *SIAM Review*, Vol. 59, 2017, pp. 849–904. <https://doi.org/10.1137/16M1062569>.
- [68] Andersson, J. A. E., Gillis, J., Horn, G., Rawlings, J. B., and Diehl, M., “CasADi – A software framework for nonlinear optimization and optimal control,” *Mathematical Programming Computation*, Vol. 11, No. 1, 2019, pp. 1–36. <https://doi.org/10.1007/s12532-018-0139-4>.
- [69] Shin, D. K., Gurdal, Z., and Griffin, O. H., “A penalty approach for nonlinear optimization with discrete design variables,” *Engineering Optimization*, Vol. 16, No. 1, 1990, pp. 29–42. <https://doi.org/10.1080/03052159008941163>.